Carbohydrate Polymers 102 (2014) 717–726

Contents lists available at ScienceDirect

Carbohydrate Polymers

journal homepage: www.elsevier.com/locate/carbpol

Reversible controlled assembly of chitosan and dextran sulfate: A new method for nanoparticle elaboration

M. Costalat, L. David, T. Delair*

Ingénierie des Matériaux Polymères, Université de Lyon, Université Lyon 1, UMR CNRS 5223 IMP, 15, Bd, A. Latarjet, Bât. Polytech, 69622 Villeurbanne Cedex, France

ARTICLE INFO

Article history:
Received 13 September 2013
Received in revised form 25 October 2013
Accepted 31 October 2013
Available online 8 November 2013

Keywords:
Chitosan
Dextran sulfate
Colloids
Reversible assembly
Polyelectrolyte complexes
Nanoparticles

ABSTRACT

Colloidal polyelectrolyte complexes (PECs) were obtained by the controlled assembly of oppositely charged dextran sulfate and chitosan, at room temperature, in water and under moderate stirring. The control over the assembly process was achieved by the slow dialysis of the sodium chloride added to the polyelectrolyte solutions prior to mixing them. This method was carried out at high polymer concentrations of 1.5 wt% and 3 wt%, with screening salt concentrations (SSC) from 2 mol L^{-1} and chitosans of degree of acetylation (*DA*) from 39% and above. The resulting particles featured a size distribution between 350 and 580 nm, a positive surface charge (30–58 mV) and remained stable for 40 days at 37 °C. The reversibility of the controlled assembly was established by adding 2 mol L^{-1} NaCl to the dispersion, the particle solubilized and then re-formed upon dialysis of the salt.

1. Introduction

Polyelectrolyte complexes are formed by mixing aqueous solutions of oppositely charged polymers. This synthesis pathway can be regarded as a green formulation process because it takes place in water, at room temperature, without any organic solvent and with a limited energy input, in comparison with methods involving an emulsification step for instance. Polyelectrolyte complexation leads to a wide variety of materials ranging from soluble complexes (Kabanov, Bronich, Kabanov, Yu, & Eisenberg, 1996; Kabanov & Zezin, 1984), through coacervates, which are complex rich liquid phases (Spruijt, Cohen Stuart, & van der Gucht, 2013), to precipitates (Chollakup, Smitthipong, Eisenbach, & Tirrell, 2010) of various morphologies such as membranes, particles fibers, etc. (Spruijt et al., 2013). The morphologies of the precipitates arise from the control of the course of the assembly via a variety of parameters, like the respective charge density and degree of polymerization of the two counterparts (Gucht, Spruijt, Lemmers, & Cohen Stuart, 2011), the polymer concentration (Schatz, Domard, Viton, Pichot, & Delair, 2004), the positive to negative charge mixing ratio (César et al., 2013), the polymer architecture (Hales & Pochan, 2006), the temperature (Chollakup et al., 2010) and ionic strength of the continuous phase (Dautzenberg, 1997; Kabanov & Zezin, 1984) and, finally, the mode of processing (Mihai, Dragan, Schwarz, & Janke, 2007).

Polyelectrolyte complexes from polysaccharides have a wide potential of application in Life Sciences, e.g. as drug delivery systems (Lankalapalli & Kolapalli, 2009), imaging tools (Hartig, Greene, Dikov, Prokop, & Davidson, 2007) or in tissue engineering (Muzzarelli, Greco, Busilacchi, Sollazzo, & Gigante, 2012), because they are based on biosourced raw materials and formulated via a green process which, *à priori*, reinforce their safety profile. Among these new materials, colloidal polyeclectrolyte complexes have received great attention as new tools for nanomedicine, using chitosan, a β (1→4) copolymer of glucosamine and *N*-acetyl glucosamine, the only naturally occurring polycation (Hamman, 2010). A great variety of anionic polysaccharides can form polyelectrolyte complexes in the colloidal size domain with chitosan, for example, carboxymethyl cellulose (Douglas & Tabrizian, 2005; Ichikawa, Iwamoto, & Watanabe, 2005), alginates (Douglas & Tabrizian, 2005), carboxymethyl konjac glucomannan (Du et al., 2005), hyaluronan and heparin (Boddohi, Moore, Johnson, & Kipper, 2009) and dextran sulfate (Delair, 2011).

The formation mechanism of chitosan–dextran sulfate colloidal polyelectrolyte complex was largely investigated: pH and ionic strength of the continuous phase, charge mixing ratio, respective molar mass of the polymer counterparts, the mode of addition were scrutinized (Schatz, Domard, et al., 2004; Schatz, Lucas, Viton, Domard, Pichot, & Delair, 2004); the stoichiometry of the complexes was found different to a 1:1 charge neutralization and

Abbreviations: Cc, critical salt concentration; SSC, screening salt concentration; CDS, complex dissociating salt; PSC, particles solid content.

* Corresponding author. Tel.: +33 04 7244 8581; fax: +33 04 7889 2583.
E-mail address: Thierry.Delair@univ-lyon1.fr (T. Delair).

0144-8617/$ – see front matter © 2013 Elsevier Ltd. All rights reserved.
http://dx.doi.org/10.1016/j.carbpol.2013.10.098

depended on the nature of the polymer used in excess (Drogoz, David, Rochas, Domard, & Delair, 2007); intrinsic parameters of chitosan, i.e. molar mass and degree of acetylation (*DA*, corresponding to the molar fraction of *N*-acetyl groups in the polymer chain) had a strong impact on the colloidal stability of the nanocomplexes (Weber et al., 2010). Interestingly, conversely to synthetic polymers, the chitosan–dextran sulfate assemblies were irreversible, i.e. the complexes would not rearrange after the addition of an excess of one of the counterparts, as a result of the cooperative interactions of hydrogen bonding and hydrophobic interactions (Schatz, Lucas, et al., 2004). But in this process, irrespective of the nature of the poly anions, the polymer concentration during the nanocomplex forming process must be low, around 0.1% by weight. This can be explained considering that the complex formation, being kinetically controlled, dilution is the only way to limit the interchain cross-linking so as to remain within the colloidal domain. This may represent a limitation for the production of larger amounts of colloidal complex and may hinder the future development of this new family of colloidal materials. Here we report for the first time a new formulation for the synthesis of colloidal polyelectrolyte complexes of chitosan, which addresses this shortcoming and which relies on the control over the polyelectrolyte chains interactions.

2. Experimental

2.1. Materials

Chitosan obtained from chitin squid pens with a relatively high weight-average molar mass and low degree of acetylation (batch 113, *DA* ~1.5%, Mw ~532 000 g mol^{-1}) was purchased from Mahtani chitosan Pvt. Ltd. Prior to use, the polymer was purified by dissolving it at 0.5% (w/v) in a stoichiometric amount of aqueous acetic acid and by filtering the resulting solution successively on membranes (Millipore) of porosity: 3, 1.2, 0.8 and 0.45 μm. Then, the polymer was precipitated with aqueous ammonia until pH 9–10. After repeated washings with de-ionized water, the neutral precipitate was freeze-dried.

The resulting chitosan purified, with a low content of GlcNAc units was *N*-acetylated to obtain a homogeneous series of samples of different *DAs*. The reaction was performed under soft conditions in a fresh solution of acetic anhydride in a water/propanediol mixture (50%/50% w/w) thus allowing the preservation of a statistical distribution of residues within the chains and the only acylation of amine functions according to Vachoud, Zydowicz, and Domard (1997). The products were isolated by precipitation on adding aqueous ammonia followed by repeated washings with de-ionized water, then freeze-dried.

Finally, hydrolysis (Schatz, Domard, et al., 2004) by controlled nitrous deamination was performed to produce low molar weight polymers. Chitosans were dissolved at 0.5% (w/v) in a 0.2 M acetic acid/0.15 M sodium acetate buffer. A 1 g/l sodium nitrite was added to chitosan solutions to obtain a nitrite/glucosamine units molar ratio of 0.1. The reaction was performed under high mechanical stirring for various times. Low molar mass chitosans were recovered by precipitation with ammonia till pH 9–10, followed by repeated washings with deionized water until neutrality and finally lyophilized.

Dextran sulfate was purchased from Sigma Aldrich and was used without further purification. The water content was determined by thermogravimetric analysis (TA Instrument TGA Q500). The molecular characteristics were determined by gel permeation chromatography, according to Schatz, Domard, et al. (2004). The degree of sulfation (the number of sulfate functions per glucosidic unit) was 2.2, as determined by colloidal titration using toluidine blue (Ueno & Kina, 1985).

Table 1
Physicochemical parameters of chitosans determined by ^{1}H NMR and SEC in an acetic acid/ammonium acetate buffer (pH 4.5).

DA (%)	Mw, $\times 10^5$ (g mol^{-1})	Ip
1.5	4.80 ± 0.05	1.8 ± 0.02
9	4.46 ± 0.05	1.7 ± 0.02
	2.73 ± 0.02	1.5 ± 0.01
	2.25 ± 0.02	1.5 ± 0.02
	0.76 ± 0.001	1.3 ± 0.02
	0.24 ± 0.001	1.2 ± 0.02
19	4.32 ± 0.05	1.5 ± 0.02
	3.08 ± 0.03	1.5 ± 0.02
	2.87 ± 0.03	1.5 ± 0.02
	1.07 ± 0.01	1.4 ± 0.02
	0.33 ± 0.02	1.2 ± 0.02
26	3.59 ± 0.05	1.7 ± 0.04
	3.24 ± 0.03	1.7 ± 0.02
	2.78 ± 0.04	1.6 ± 0.05
	1.02 ± 0.01	1.4 ± 0.04
	0.37 ± 0.003	1.3 ± 0.02
27	4.96 ± 0.06	1.6 ± 0.05
	3.14 ± 0.08	1.6 ± 0.07
	1.04 ± 0.07	1.3 ± 0.02
	0.32 ± 0.01	1.2 ± 0.06
32	4.33 ± 0.05	1.5 ± 0.05
33	4.83 ± 0.06	1.5 ± 0.04
39	4.58 ± 0.05	1.7 ± 0.05
	3.51 ± 0.03	1.7 ± 0.02
	3.00 ± 0.02	1.6 ± 0.02
	1.33 ± 0.03	1.4 ± 0.05
	0.52 ± 0.06	1.2 ± 0.1
47	3.96 ± 0.04	1.7 ± 0.03
	1.88 ± 0.04	1.7 ± 0.05
	1.49 ± 0.05	1.5 ± 0.08
	0.52 ± 0.02	1.2 ± 0.06
50	4.62 ± 0.09	1.6 ± 0.03
	3.04 ± 0.04	1.6 ± 0.03
	2.73 ± 0.04	1.6 ± 0.04
	1.78 ± 0.03	1.5 ± 0.04
	0.74 ± 0.001	1.2 ± 0.02

2.2. Methods

2.2.1. Characterization of chitosan

The degree of acetylation was determined by ^{1}H NMR spectroscopy (Brucker Avance III 400 MHz) at 25 °C. Samples were prepared by dissolving 10 mg of chitosan in 1 mL of D2O and 5 μl of HCl. The *DA* value was calculated according to the Hirai et al. method.

The water content was determined by thermogravimetric analysis (TA Instrument TGA Q500). The weight average molar mass Mw and the polydispersity indexes (Ip) were measured by size exclusion chromatography (2500 and 6000 PW TSK gel columns from Tosohaas) coupled online with a differential refractometer (Wyatt Optilab T-rEx) and a multiangle laser light scattering detector (Wyatt Dawn EOS) operating at λ = 633 nm. A degassed 0.2 M acetic acid/0.15 M ammonium acetate buffer with a pH 4.5 was used as the eluent. The flow rate was maintained at 0.5 ml/min. The refractive index increments (dn/dc) were added independently for each degree of acetylation according to a previous study (Schatz et al.). The physicochemical parameters of the chitosan samples are reported in Table 1.

2.2.2. Preparation of polyelectrolytes solutions in presence of different sodium chloride concentrations

Taking into account the initial water content, chitosan was dispersed at various concentrations with a stoichiometric amount of aqueous acetic acid with respect to the free amines group for each chosen degree of acetylation. Dissolution was achieved after overnight stirring. Then, sodium chloride was added to each solution to obtain the expected concentration. Dextran sulfate

solutions, at different concentration were prepared in deionized water. Sodium chloride was also added to obtain the same concentration as in chitosan solutions. Then polyelectrolytes and sodium chloride were mixed and stirred for 2 h.

2.2.3. Polyelectrolytes solubility in salt solution

The solubility of the polyelectrolytes in presence of different concentration of sodium chloride was characterized by absorbance measurement at $\lambda = 400$ nm with an UV/vis spectrometer (Perkin Elmer Instruments Lambda 35). At this wavelength chitosan and dextran sulfate did not absorb. Deionized water was used to establish the baseline. Absorbance values were expressed as the average of three independent measurements.

2.2.4. Chitosan intrinsic viscosity

Various chitosan solutions were prepared as above. Then, these solutions were filtered through 0.45 μm and injected into an Ubbelohde tube capillary viscometer (Viscologic TI.1, SEMATech) with an inner diameter of 0.53 mm and equipped with an automatic dilution (±0.05%). Measurements were achieved at 25 °C using deionized water and acetic acid (with the same proportion as in the solution of chitosan) as reference to establish the viscosity of the pure solvent. The intrinsic viscosities were determined by extrapolating the reduced viscosity to zero concentration.

2.2.5. Small angle X-ray scattering

Small angle X-ray scattering (SAXS) experiment was performed at the European Synchrotron Radiation Facility (Grenoble, France) on the BM2-D2AM beamline. The samples of chitosan (0.25% (w/v)) dispersed in salt solution (0, 2, and 6 M) obtained as described above were installed in silica tubes (external diameter 3 mm, wall thickness 0.2 mm, 76 mm long, from Deutero GmbH, ref. 2000942) with elastomer closure caps to avoid water evaporation (Deutero ref. 29 604 15). The incident photon energy was set to 16.000 kev to limit attenuation by the glass tubes.

We used a 2D CCD X-ray detector from Ropper scientific. The images were corrected for camera distortion, dark image reading and flat field response of the detector. Finally, the image center ("gravity center" of the incident beam) was determined with attenuators and radial averages yielded 1D profiles (processing carried on the beamline, with bm2img software). The scattering angle (2θ) or q-calibration ($q = 4\pi \sin(\theta)/\lambda$) was performed thanks to a silver behenate powder standard placed in a glass tube in the 21-sample holder. The subtraction of the scattering contribution of the empty cell (glass tube filled with the corresponding aqueous saline solution without chitosan) was performed by measuring the attenuation coefficient of the samples. The analysis of the data is carried out by a Levenberg–Marquardt nonlinear regression routine using Octave and least square function.

2.2.6. Polyelectrolyte complex formation by controlled association

The method is summarized in Fig. 1. Various concentrations of chitosan samples soluble at all salt concentration were prepared in deionized water as above. The pH was adjusted to 4.0 with 0.1 M acetic acid or 0.1 M sodium hydroxide. Then, sodium chloride was added at various concentrations to screen the polyelectrolyte charge by chloride ions. Dextran sulfate solutions, at different concentrations were prepared directly in deionized water, pH was adjusted to 4.0 and sodium chloride was added at the appropriate concentrations.

Appropriate volumes of the above solutions were mixed so as to the charge mixing ration $R = 2$ ($n+/n-$ molar mixing ratios between cationic and anionic charges) under a constant magnetic stirring of 800 rpm. This solution was then dialyzed against deionized water (Spectra/Por® membrane, MWCO = 3500 g mol^{-1}) to progressively

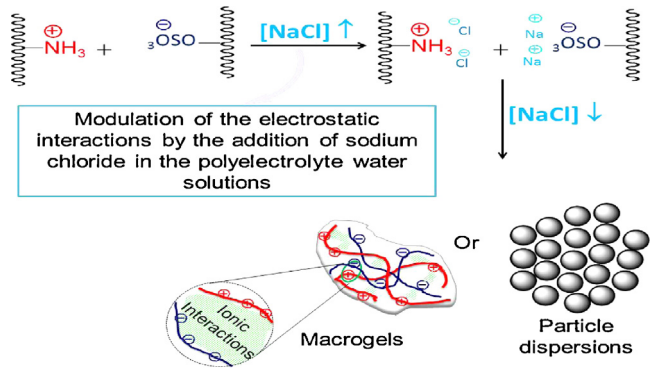

Fig. 1. Polyelectrolyte complexation process by controlled association.

eliminate sodium chloride. The dialysis bath ($V = 100$ times the volumes of the polymer solution) was changed every hour during the three first hours. It was then changed every 2 h until the end of the dialysis duration (16 h).

Another dialysis method was used, called here 'soft dialysis'. Instead of using water the dialysis bath contained 500 mmol L^{-1} salt. This salt concentration was then decreased by half every hour at the time of water changing to reach a zero concentration. The end of dialysis was realized as previously described.

2.2.7. Dialysis kinetics

The chloride ions content was monitored with time by potentiometric titration (TitraLab TIM865, Radiometer Analytical) using a 0.1 N $AgNO_3$ as titrant and two or three nitric acid drops to avoid the formation of metallic hydroxide. The end of dialysis was determined by the absence of chloride ions in the water of the dialysis bath.

2.2.8. Physicochemical characterization of the complex dispersions

2.2.8.1. Particle solid contents. Particles were separated from the aqueous phase by centrifugation at 23 000 g for 1 h. The supernatant was carefully discarded, and the pellet was dried at 60 °C overnight. The solid content was defined by the ratio between the dried particle weight to the weight of the dispersion.

2.2.8.2. Quasi-elastic light scattering. Dynamic light scattering measurements were performed on a Malvern Zetasizer ZS equipped with a 5 mW He/Ne laser beam operated at $\lambda = 633$ nm and at 173° scattering angle. The self-correlation function was expanded in a power series (Cumulants method). Size values are the average of 3 series of five measurements obtained at 25.0 ± 0.2 °C.

2.2.8.3. Electrophoretic mobilities. The electrophoretic mobilities were determined at 25.0 ± 0.2 °C with a Malvern Zetasizer ZS equipped with a 5 mW He/Ne laser at $\lambda = 632.8$ nm. The electrophoretic mobility was expressed as the average of ten measurements. Before measurement, particles were dispersed in deionized water.

2.2.8.4. Transmission electron microscopy. Morphology and the shape of chitosan–dextran sulfate particles were examined using transmission electron microscopy (PHILIPS CM120). A droplet of 0.01% (v/v) particle dispersion was deposited on a copper grid covered with carbon film. The excess water was removed by blotting with filter paper, and then air dried at room temperature. The observation was occurred using an accelerating voltage of 80 kV.

2.2.8.5. Cryo-transmission electron microscopy. For cryo-TEM experiments, a droplet of 1.5% (v/v) particle dispersion was put on

an advanced holey carbon film coated on copper grid. The excess water was removed by blotting with filter paper and subsequently the grid was vitrified by plunging it into liquid ethane cooled by liquid nitrogen thus forming a thin film of solid amorphous water. The cryo holder was then transferred into the vacuum column of TEM microscope (PHILIPS CM120) maintained at liquid nitrogen temperature for the observation at120 kV voltage. Both TEM and Cryo-TEM experiments were carried out at the Center Technologique des Microstructures – Université Claude Bernard Lyon 1.

2.2.9. Reversibility of the controlled polyelectrolyte complexation method

To study the reversibility of the controlled complexation method, salt was added to the particles dispersions to obtain various concentrations. For particular salt contents, clear solutions were obtained and then, they were dialyzed as previously described to form complex particles once again. This operation was repeated several times to study the impact of this reversibility on particles sizes.

3. Results and discussion

The control over the complexation of the two polyelectrolytes was achieved by adding a low molecular weight electrolyte at a concentration that enabled total charge screening. First, the impact of the presence of salt on the water solubility of chitosan and on the conformation of the polymer was investigated.

3.1. Impact of salt concentration on the water solubility of chitosan. Effects of DA polymer concentration and chitosan Mw

For this investigation a large variety of chitosan samples were synthetized, whose degrees of acetylation and molar masses are reported in Table 1. Chitosan solutions of varying ionic strength were prepared and the solubility was checked by measuring the absorbance. At low salt concentration each solution was homogenous, but on increasing the NaCl concentration, a desolvation of the polymer took place at a critical NaCl concentration, depending on the intrinsic properties of chitosan and also the polymer concentration in solution.

In Figs. 2 and 1-SD are reported the absorbance variations with increasing salt concentrations for various *DAs* and polymer concentrations, for a fixed molar mass of 400 kg mol^{-1} (Fig. 2) and at constant concentration (0.5% (w/v)) but with varying molar masses (Fig. 1-SD). For a critical salt concentration (Cc), the absorbance sharply increased to a plateau value, which corresponded to the total precipitation of the polymer. Three major observations can be made from these Figs. 2 and 1-SD: (i) first, there is a limit value in *DA*, *DA* = 39%, above which chitosan remained soluble irrespective of the salt concentration; (ii) second, the value of the critical salt concentration decreased with increasing polymer concentration;

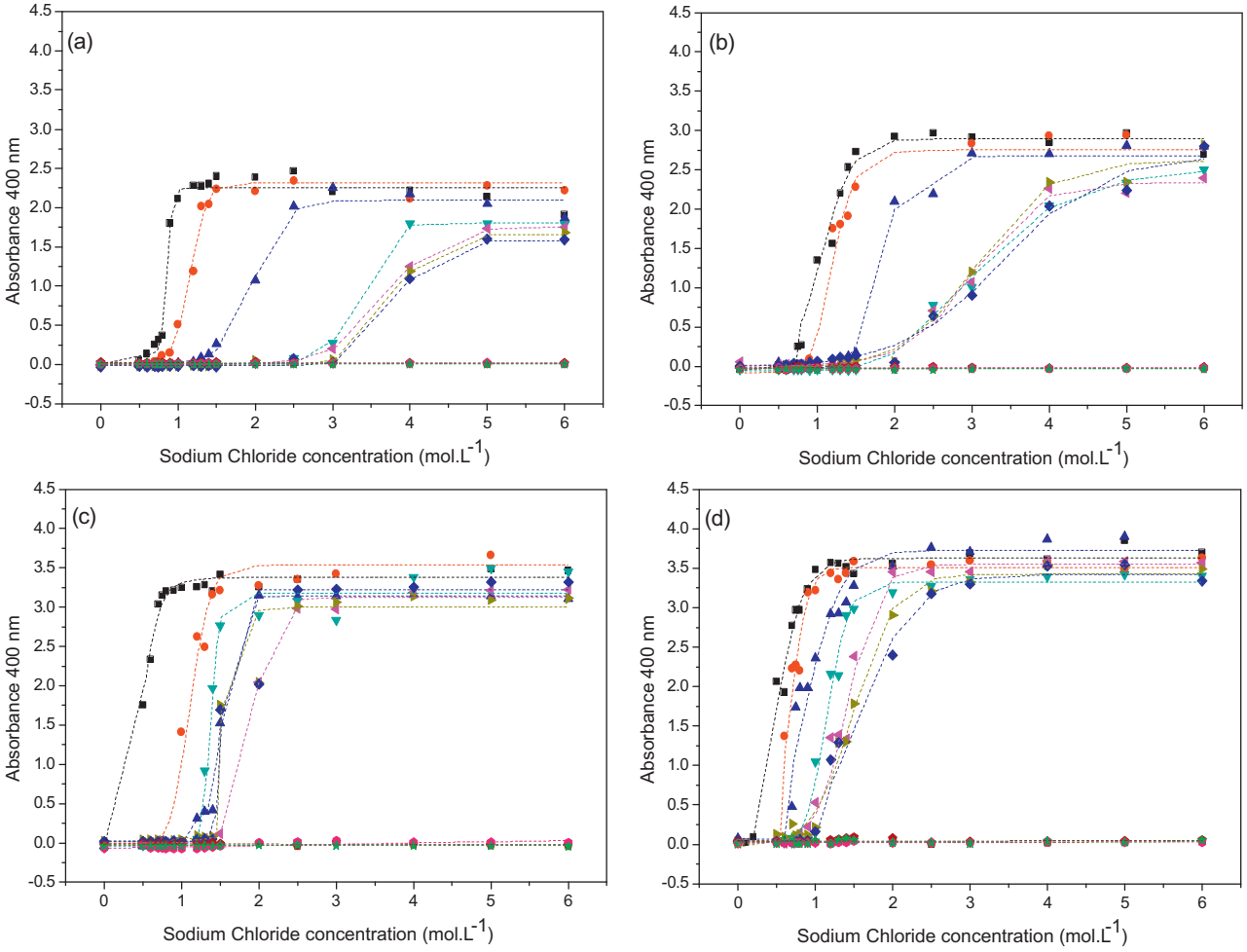

Fig. 2. Absorbances (λ = 400 nm) of chitosan solutions as a function of NaCl concentration for a fixed molar mass (ca 400,000 g mol^{-1}), at various polymer concentration and degree of acetylation: (a) *CS* 0.25%, (b) *CS* 0.5%, (c) *CS* 1.5%, (d) *CS* 3%. ■ *DA* = 1.5%, ● *DA* = 9%, ▲ *DA* = 19%, ▼ *DA* = 26%, ◀ *DA* = 27%, ▶ *DA* = 32%, ◆ *DA* = 33%, ⬟ *DA* = 39%, ● *DA*= 47%, ★ *DA* = 50%.

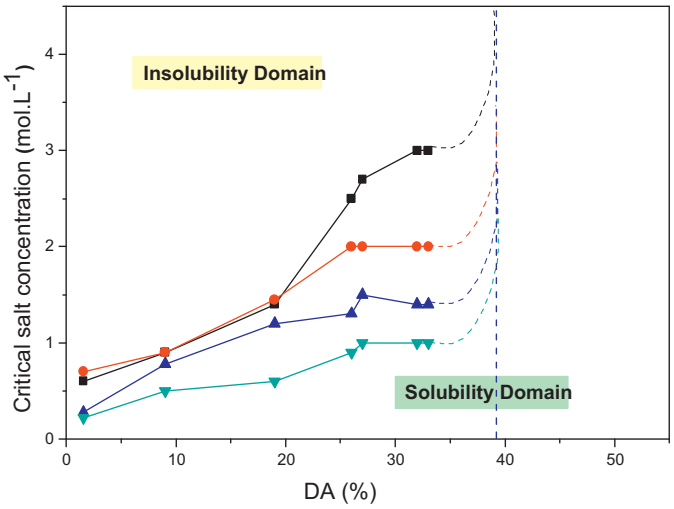

Fig. 3. Solubility diagram of chitosan as a function of *DA*, for salt concentration: (■) *CS* = 0.25% (w/v), (●) *CS* = 0.5% (w/v), (▲) *CS* = 1.5% (w/v), (▼) *CS* = 3% (w/v).

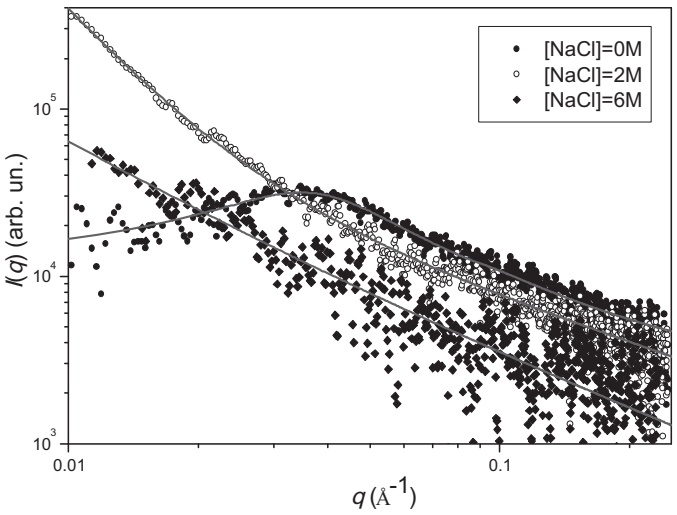

Fig. 4. The evolution of $I(q)$ detected with chitosan solution at 0.25% (*DA* 50%) and different salt concentrations (lines are graphic guides for the eye using a Lorentzian curve for $I(q)$ at [NaCl] = 0 M; and a generalized Porod's law $I(q) = C/q^{\alpha}$ with $\alpha = f(q)$ for [NaCl] = 2 M and 6 M).

(iii) third the molar mass of chitosan had a limited impact on the value of the this critical concentration.

The existence of a limit *DA* of 39% above which chitosan remained soluble (see Fig. 2-SD of Supplementary Data) can be related to its solution properties described in the law of behavior of chitosan solutions (Schatz, Viton, Delair, Pichot, & Domard, 2003). At low *DA*, chitosan is a polyelectrolyte due to the protonation of the amine groups and the solubility of the polymer chain depend on the existence of electrostatic repulsive forces that repel the polymer chain from one another and expand the polymer chain. Screening these electrostatic forces favor the inter or intra chain interactions via hydrogen bonding, hence the observed desolvation process. At higher *DAs*, the electrostatic charge density on the polymer chains decreased to the profit of polar *N*-acetyl groups, capable of hydrogen bonds with water. Hydrogen bonding is less sensitive to ionic strength and so the polymer remains soluble at high salt concentration. This is confirmed by the fact that the critical salt concentration increased with *DA*, at constant molar mass (Fig. 3). Interestingly, the increase in Cc is sharp till *DA* = 25% and then plateaued till 39%. This change in slope can be related to the difference in behavior of chitosan in solution, a strong polyelectrolyte below *DA* 25% dominated by electrostatic interactions, and a mixed behavior above, where electrostatic effects are counterbalanced by Van der Waals interactions, in accordance with the law of behavior (Schatz et al., 2003).

As would be expected, Cc decreased with increasing concentration of chitosan in solutions and the effect was more marked at higher *DAs* than at lower *DAs* for which electrostatic effects predominated and the polymer precipitated out at low salt concentrations. More unexpectedly was the lack of effect of molar mass on the value of the critical salt concentration. As seen from Fig. 1-SD, the onset of the phase separation was identical for each molar mass for a set value of *DA*. Similarly, the *DA* limit value at which chitosan samples remained soluble irrespective of the salt content in the aqueous phase *DA* = 39%, was independent of the degree of polymerization of the chitosan chains.

In contrast to chitosan, dextran sulfate samples remained soluble for each salt concentration and molar mass, in the investigated concentration range (Fig. 3-SD of Supplementary Data). This behavior can be attributed to the high flexibility of the dextran chains imparted by the α1→6 glycosidic bond to the high degree of substitution of dextan sulfate (DS = 2.2)

The effect of the screening of electrostatic interactions on the conformation of chitosan in solution can be viewed at the macroscopic level on the value of the intrinsic viscosity of chitosan as a function of the ionic strength, expressed in NaCl concentration. With increasing salt concentration in water, the viscosity dropped sharply to level off for a salt concentration of 1 mol L^{-1}, suggesting that this concentration would be sufficient to screen electrostatic interactions (Fig. 3-SD). Interestingly, the lower the *DA*, the lower the intrinsic viscosities (see insert of Fig. 3-SD-a), which is correlated to the polyelectrolyte nature of chitosans of low *DAs*, for which electrostatic interactions predominate. The effect of the degree of polymerization of chitosan can be observed in the insert of Fig. 3-SD-b, where the intrinsic viscosity of the lower molar mass chitosan is lower than for the higher one, as would be expected. Clearly, the behavior of chitosan is greatly dependent on the molar fraction of *N*-acetyl groups in the polymer chain, similarly to its solubility as a function of the electrolyte concentration.

The small angle X-ray scattering data of Fig. 4 confirmed the change in nature of the solutions, the polyelectrolyte peak detected in the absence of salt), corresponding to an order due to electrostatic interactions (Boucard et al., 2007; David et al., 2005), was no longer well detected in the presence of 2 and 6 mol L^{-1} sodium chloride. For these salt concentrations, at low q values, one can observe the presence of macromolecular aggregates as described by Popa-Nita, Alcouffe, Rochas, David, and Domard (2009). The difference in signal intensity for the 2 and 6 mol L^{-1} sodium chloride solutions was due the attenuation from chloride ions.

3.2. Conditions of the complexation process by controlled assembly

The mixing of the chitosan and the dextran sulfate solutions at increasing salt concentrations lead to a macrogel for salt concentrations lower than 1 mol L^{-1}, or dispersed precipitates for a concentration range of 1 to 2 mol L^{-1} (Fig. 5). For a salt content of 2 mol L^{-1} and higher, the solutions remained homogenous without any phase separation. Hence, to achieve a screening of the electrostatic interactions sufficient enough to prevent phase separation, at least a 2 mol L^{-1} NaCl concentration was required. This salt concentration is higher than that required for the assembly of inorganic nanoparticles with macromolecules as reported by Fresnais, Lavelle, and Berret (2009) and Yan, Fresnais, and Berret (2010). This difference can be attributed to the difference in starting materials, these investigators used nanoparticles and synthetic

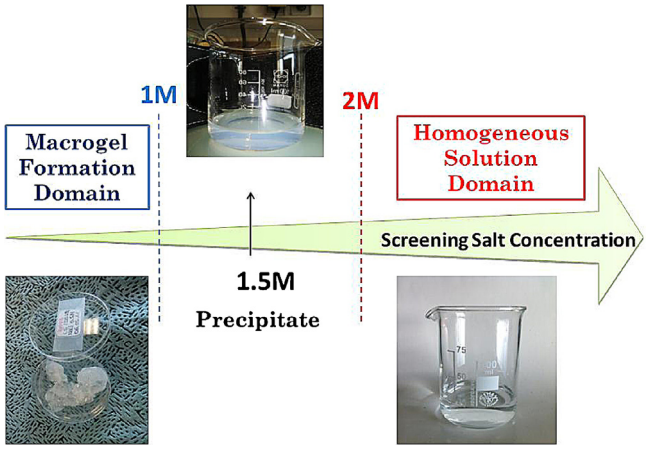

Fig. 5. Effect of the sodium chloride concentration on the mixing of chitosan and dextran sulfate solutions.

polymers whose nature of electrostatic charges was quite different than ours and, also, the hydrocarbon backbone of their macromolecules was more flexible than the β, 1→4 glycosidic bond of chitosan.

3.3. Formation of polyelectrolytes complex dispersions

The homogenous mixtures were dialyzed against deionized water and the monitoring of the release of the chloride ions was achieved by conductometric titration using silver nitrate and a silver specific electrode. The kinetics of the chloride elimination was moderately impacted by the salt concentration as seen in Fig. 6a, as 100% of chloride ions were eliminated in 5 or 6 h for starting concentrations in sodium chloride of 2 or 6 mol L^{-1}, respectively.

An increase in the chitosan concentration of the solution to be dialysed resulted in an increase in dialysis time to reach 100% elimination of chloride ions (compare Fig. 6a and b) for the 6 mol L^{-1} NaCl concentration and to a lesser extend for the 2 mol L^{-1} concentration. The increase in viscosity of the chitosan solutions with increasing polymer concentration can account for this observation.

The controlled complexation process between chitosan and dextran sulfate was shown to be reversible, on adding to a colloidal dispersion the appropriate amount of sodium chloride to reach a salt concentration of 2 mol L^{-1}, the particles re-dissolved to a limpid solution (Fig. 4-SD). Dialysing this solution against water provided, again, a colloidal dispersion of polyelectrolyte complex.

In Table 2 we show the results on the reversibility of the process and the impact of the number of re-dissolution/re-dialysis cycles on particle sizes, for a salt concentration used for re-dissolution ranging from 2 to 6 mol L^{-1} and for two chitosan concentrations 1.5% and 3%. First, it is worth noting that, on increasing the sodium chloride concentration for screening, the particle size decreased as a result of a slower kinetics of ion pair association, favoring a more compact conformational adaptation of the macromolecules. After three dissolution/dialysis cycles, the particle size stabilized around 300 nm, suggesting that after synthesis the particles were not stable thermodynamically and could undergo rearrangements. Going through these three cycles, particle zeta potential also decreased, suggesting that the compaction of the particles resulted from a higher level of charge neutralization by ion pairing. We will come back to that kinetics versus thermodynamic control of particles size in Section 3.4 in this paper. Anyhow, one can conclude that the particle formation process is totally reversible.

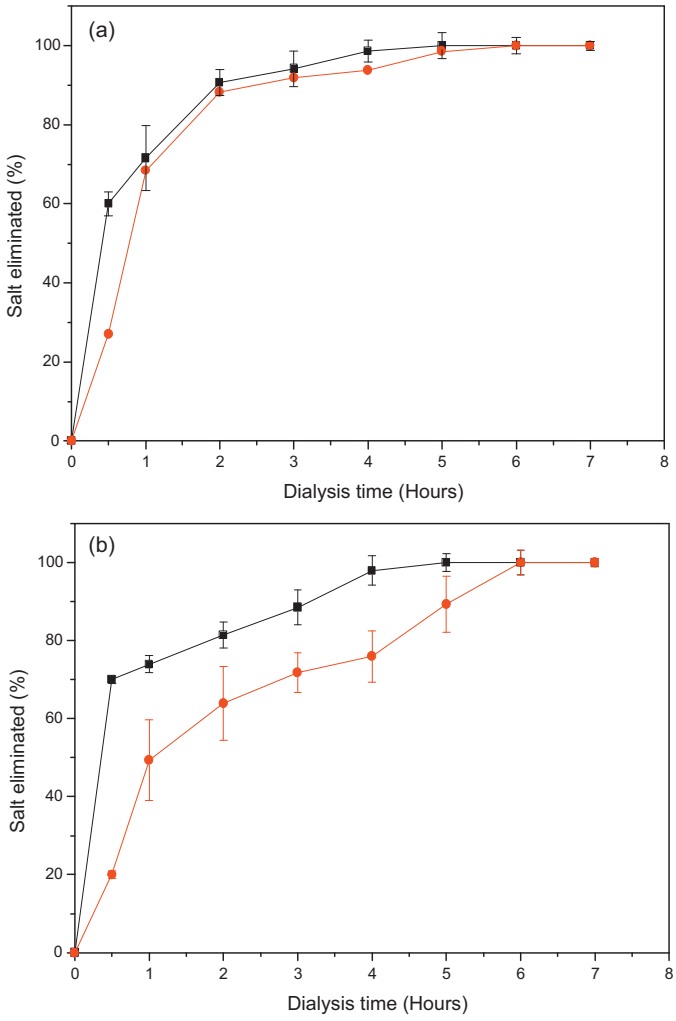

Fig. 6. Dialysis kinetics by monitoring the concentration of released chloride ions. Polymer concentration (a) 1.5% and (b) 3%. ■ NaCl = 2 mol L^{-1}, ● NaCl = 6 mol L^{-1}.

3.4. Colloidal characterization of the complexes and colloidal stability

Particle sizes were measured after dialysis and after storing in deionized water (Fig. 5-SD) or in a 50 mmol L^{-1} sodium chloride aqueous solution (Fig. 7) at 37 °C or room temperature. The dispersions were obtained by dialysis of mixtures containing from 2 mol L^{-1} to 6 mol L^{-1} sodium chloride. The observed general trend was a decrease in particle size from $t = 0$, i.e. after dialysis, and $t = 5$ days or more, depending on the storing conditions. In water, storing the particles at 37 °C lead to smaller particle sizes than at room temperature, though the effect was less marked as the initial salt concentration before dialysis increased, and for 6 mol L^{-1} the two curves superimposed. When the dispersions were stored in the presence of 50 mmol L^{-1} sodium chloride, the particles had similar sizes, irrespective of the storing temperature but, after 15–20 days at room temperature, the particles aggregated irreversibly, whereas they remained stable at 37 °C.

These results show that the objects resulting from the controlled charged neutralization were not at equilibrium after dialysis and could undergo reorganizations. In the absence of salt in the storing medium, the reorganization was slower, or more limited in range, at room temperature than at 37 °C. In the presence of salt, the reorganizations seemed to occur at similar rates for both temperatures till the flocculation took place at days 15–20 for dispersions stored at

Table 2
Process reversibility: size and surface charge of chitosan/dextran sulfate nanoparticles obtained after up to three dissolution/dialysis cycles.

Dissolution/dialysis cycle[a]	CDS[b] (mol L^{-1})	Size (nm)	PI	Zeta potential (mV)
Particles at 1.5% solid content				
0	2	1152	0.2	+53
	3	1128	0.2	+54
	4	1069	0.2	+55
	5	1022	0.2	+52
	6	743	0.1	+55
1	2	565	0.2	+38
	3	531	0.2	+38
	4	399	0.2	+39
	5	355	0.2	+37
	6	325	0.1	+33
2	2	489	0.2	+34
	3	347	0.1	+33
	4	333	0.1	+32
	5	343	0.1	+22
	6	350	0.1	+22
3	2	315	0.1	+27
	3	313	0.1	+23
	4	321	0.1	+20
	5	338	0.1	+22
	6	298	0.1	+23
Particles at 3% solid content				
0	2	1593	0.2	+58
	3	1524	0.2	+55
	4	1265	0.2	+55
	5	1226	0.2	+57
	6	1018	0.1	+57
1	2	930	0.2	+53
	3	848	0.2	+54
	4	722	0.2	+54
	5	678	0.2	+55
	6	734	0.2	+56
2	2	839	0.2	+47
	3	559	0.2	+47
	4	453	0.2	+45
	5	265	0.1	+48
	6	259	0.1	+38
3	2	685	0.2	+47
	3	483	0.2	+47
	4	314	0.2	+46
	5	258	0.1	+47
	6	251	0.1	+42

[a] Cycle 0 means particles formed for the first time by mixing polysaccharide solutions and dialysis.
[b] CDS, complex dissociating salt.

room temperature. These reorganizations suppose the destruction of some ion pairs, earlier formed in the elaboration process, and the formation of new ones leading to more compact complexes. In these new structures, the macromolecules underwent conformational adaptation to increase the charge neutralization within the complexes. The conformational adaptation was favored by an energy input and also by a partial screening of electrostatic interaction with salt. This screening increased the reversibility of the ion-pairing process, selecting the ion-pairs associated with less steric constraints. The systematic flocculation observed at room temperature after 15–20 days of storing is not yet fully understood. Nevertheless, it can be attributed to interfacial reorganizations of the polymer chains, theses conformational rearrangements leading to a loss of colloidal stability. At 37 °C, one can speculate that the increased chain mobility prevented such a reorganization to occur so, the interfacial chitosan chains could still ensure the electrosteric stability of the colloids.

In the preceding experiment we did not report any storing at +4 °C because at this temperature, particles aggregated very quickly, see Table 3(a). But, for further applications in Life Sciences, in which these particles will be associated with temperature labile biological molecules, it will be essential to store them at +4 °C. To this end, we modified the dialysis procedure to slow down the desalting process: in the dialysis bath, we substituted deionized water by a solution containing 500 mmol L^{-1} NaCl. Moreover, this salt concentration was decreased by half every hour to reach a zero concentration. The particles obtained by this 'soft dialysis' technique ('soft' because the desalting kinetics of the polyelectrolyte solution was slower than when de-ionized water was used from the start of the process) were colloidally stable up to 2 years when stored at +4 °C, as reported in Table 3(b). These results confirm that the control of the kinetics of salt elimination is a key factor, greatly impacting the properties of the final colloids. This is consistent with our results reported in Figs. 5-SD and 7 which showed that the kinetically obtained objects could re-organize into more stable assemblies. Data in Table 3(b) also confirm that (i) particles after synthesis had a large average size and reorganized with time into smaller objects; (ii) particles obtained with 6 mol L^{-1} sodium chloride were more compact than those obtained from 2 mol L^{-1}, the differences being less marked with the soft dialysis method.

The spherical morphology of the colloidal complexes was confirmed by two different microscopy techniques, namely transmission electron microscopy and cryo-transmission electron microscopy (Fig. 8). Fig. 8a shows particles obtained before the reorganization process was complete, the particles were associated to one another. In Fig. 8b and c, we clearly observed the reorganization that took place overtime for two different solid content: the colloidal assemblies appeared as single particles throughout the

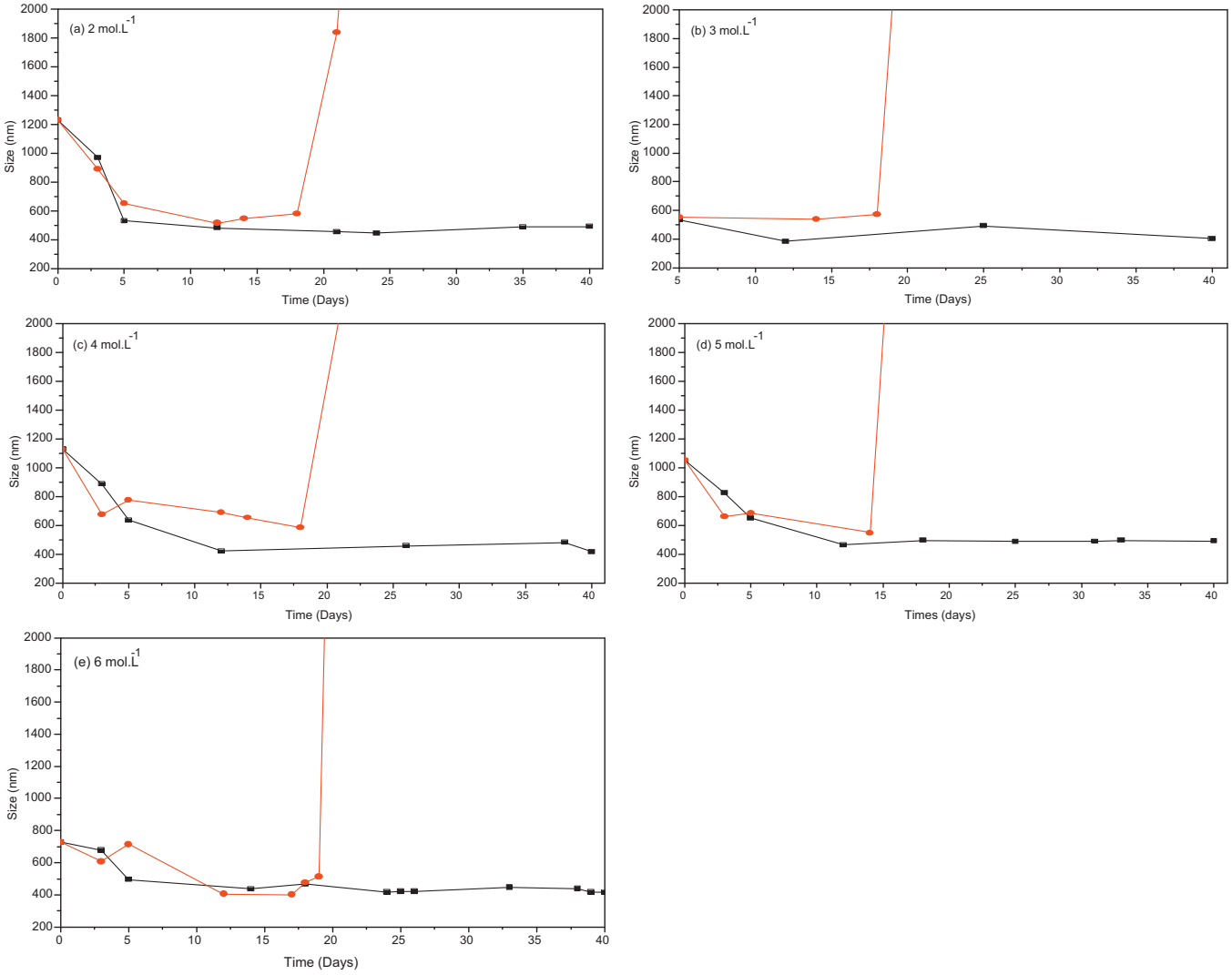

Fig. 7. Colloidal stability over time for dispersions stored in a 50 mmol L^{-1} aqueous solution (solid content = 1.5%). ■ 37 °C; ● RT.

Table 3
Size and surface charge of particles dispersed in water and stored at +4 °C as function of dialysis method used: dialysis against water and soft dialysis (chitosan DA 49%, Mw 133, 000 g mol^{-1}; dextran sulfate Mw 12.86 × 10^5 g mol^{-1} and sulfate content 2.1).

SSC (mol L^{-1})	Time		Day 0	Day 10		2 years			
	Size (nm)	PI	Zeta potential (mV)	Size (nm)	PI	Zeta potential (mV)	Size (nm)	PI	Zeta potential (mV)
Particles obtained by dialysis against deionized water									
PSC 1.5%									
2	1144	0.2	+54	Floculation			–	–	–
6	727	0.2	+58	Floculation			–	–	–
PSC 3%									
2	1292	0.20.2	+51	Floculation			–	–	–
6	968		+61	Floculation			–	–	–
Particles obtained by soft dialysis									
PSC 1.5%									
2	1285	0.2	+52	477	0.2	+54	579	0.2	+55
6	1260	0.2	+55	324	0.1	+54	549	0.1	+55
PSC 3%									
2	1526	0.2	+55	919	0.2	+59	567	0.2	+46
6	1423	0.1	+55	613	0.2	+59	544	0.2	+46

PSC, particles solid content.

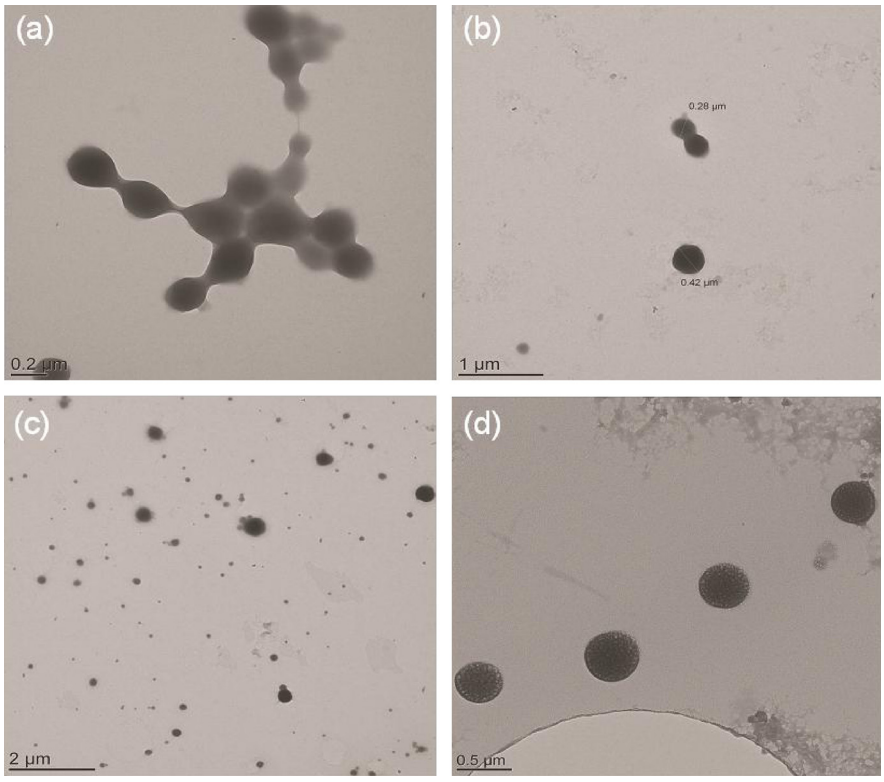

Fig. 8. Transmission electron microphotography of particles in water obtained from 1.5% on solid content: (a) 5 days after dialysis, (b) 15 days after dialysis, and (c) from 3% of solid content after stabilization. (d) Cryo-transmission electron microphotography at 1.5% of solid content (chitosan *DA* 49%, Mw 130,000 g mol^{-1}; *DS*, Mw 12.86 × 10^5 g mol^{-1} and sulfate content 2.2).

samples. In order to reduce the impact of sample preparation on the morphology of the particles, the same colloidal suspensions were analyzed by cryo-transmission electron microscopy, Fig. 8d, confirming the spherical shape of the objects. However, upon exposure to the electron beam, the particles quickly degraded which explains the non-uniformity of the particle internal structure.

4. Conclusion

Colloidal polyelectrolyte complexes were obtained via a controlled assembly process, based on the screening of electrostatic interactions between oppositely charged polysaccharides using an adequate concentration of electrolyte in the medium.

The presence of salt in the chitosan solution induced a desolvation of the polymer at a critical salt concentration (Cc), whose value was directly impacted by the degree of acetylation of chitosan. We evidenced a limit *DA* of 39% above which chitosan remained soluble, whatever the electrolyte concentration. The impact of the *N*-acetyl groups content on the water solubility of chitosan in the presence of salt was attributed to (i) the charge density decreased, with increasing *DA*, hence reducing the polyelectrolyte character of the macromolecules, (ii) a concomitant increase in the polarity of the macromolecules favoring its capability at forming hydrogen bonds with water. In contrast, dextran sulfate remained soluble, irrespective of the salt concentration. These differences in behavior were attributed to macromolecular characteristics of the poly ions: a flexible α1→6 dextran sulfate with a degree of substitution of 2.2 and a rigid β1→4 chitosan, prone to associate inter molecularly by hydrogen bonding.

Mixing of the polyelectrolyte solutions at a salt concentration of 2 mol L^{-1} or higher, yielded a homogenous liquid phase which upon dialysis against water could allow the self assembly of the polyelectrolytes into colloidal particles of dextran sulfate–chitosan complexes. This complexation process was shown to be reversible, adding to the dispersions sodium chloride up to 2 mol L^{-1}, the particles re-dissolved to a limpid solution.

The colloidal complexes obtained from this controlled process underwent macromolecular reorganizations over time, leading to more compact particles. The variations in colloidal stability with the external parameters like temperature and salt concentration were attributed to the reversibility of these associations. One of the most important conclusions of this work is that it is essential to decrease the kinetic control of the particle formation process to favor, using high salt concentration and slow dialysis kinetics, a thermodynamically controlled process. Further work will address the evaluation of (i) the scope of this process versus other polyanions; (ii) the interfacial functionalization of these nano complexes with proteins or ligands for drug targeting of vaccine delivery; (iii) the loading of these colloidal complexes with active molecules.

Acknowledgments

The authors would like to acknowledge Pierre Alcouffe and the Centre Technologique des Microstructures – Université Claude Bernard Lyon 1 (http://microscopies.univ-lyon1.fr/) for their expertise and assistance in electron microscopy. We also are in debt to Jean-Michel Lucas and Agnès Crépet for their expertise and assistance in molar mass determination by SEC. This work was financed by the ANR project PECSDDeli. MC is grateful to the ANR project PECSDDeli for attributing her PhD grant. We also thank all the BM2-D2AM staff for the help and various expertise during the SAXS/WAXS experiments at ESRF

Appendix A. Supplementary data

Supplementary data associated with this article can be found, in the online version, at http://dx.doi.org/10.1016/j.carbpol.2013.10.098.

References

Boddohi, S., Moore, N., Johnson, P. A., & Kipper, M. J. (2009). Polysaccharide-based polyelectrolyte complex nanoparticles from chitosan, heparin, and hyaluronan. *Biomacromolecules*, *10*(6), 1402–1409.

Boucard, N., David, L., Rochas, C., Montembault, A., Viton, C., & Domard, A. (2007). Polyelectrolyte microstructure in chitosan aqueous and alcohol solutions. *Biomacromolecules*, *8*(4), 1209–1217.

César, M.-B., Castañeda, L., Enciso-Aguilar, M., Gerardo, P.-Q., Heriberto, A.-C., Amir, M.-A., et al. (2013). Structure and mechanism formation of polyelectrolyte complex obtained from PSS/PAH system: Effect of molar mixing ratio, base–acid conditions, and ionic strength. *Colloid and Polymer Science*, *291*, 683–690.

Chollakup, R., Smitthipong, W., Eisenbach, C. D., & Tirrell, M. (2010). Phase behavior and coacervation of aqueous poly(acrylic acid)–poly(allylamine) solutions. *Macromolecules*, *43*(5), 2518–2528.

Dautzenberg, H. (1997). Polyelectrolyte complex formation in highly aggregating systems. 1. Effect of salt: Polyelectrolyte complex formation in the presence of NaCl. *Macromolecules*, *30*(25), 7810–7815.

David, L., Montembault, A., Vizio, N., Crépet, A., Viton, C., Domard, A., et al. (2005). Ordering in bio-polyelectrolyte chitosan solutions. *Macromolecular Symposia*, *222*(1), 281–286.

Delair, T. (2011). Colloidal polyelectrolyte complexes of chitosan and dextran sulfate towards versatile nanocarriers of bioactive molecules. *European Journal of Pharmaceutics and Biopharmaceutics*, *78*(1), 10–18.

Douglas, K. L., & Tabrizian, M. (2005). Effect of experimental parameters on the formation of alginate-chitosan nanoparticles and evaluation of their potential application as DNA carrier. *Journal of Biomaterials Science-Polymer Edition*, *16*(1), 43–56.

Drogoz, A., David, L., Rochas, C., Domard, A., & Delair, T. (2007). Polyelectrolyte complexes from polysaccharides: Formation and stoichiometry monitoring. *Langmuir*, *23*(22), 10950–10958.

Du, J., Sun, R., Zhang, L. F., Zhang, L. F., Xiong, C. D., & Peng, Y. X. (2005). Novel polyelectrolyte carboxymethyl konjac glucomannan-chitosan nanoparticles for drug delivery. I. Physicochemical characterization of the carboxymethyl konjac glucomannan-chitosan nanoparticles. *Biopolymers*, *78*(1), 1–8.

Fresnais, J., Lavelle, C., & Berret, J. F. (2009). Nanoparticle aggregation controlled by desalting kinetics. *Journal of Physical Chemistry C*, *113*(37), 16371–16379.

Gucht, J., Spruijt, v. d., Lemmers, E., & Cohen Stuart, M. M. A. (2011). Polyelectrolyte complexes: Bulk phases and colloidal systems. *Journal of Colloid and Interface Science*, *361*(2), 407–422.

Hales, K., & Pochan, D. J. (2006). Using polyelectrolyte block copolymers to tune nanostructure assembly. *Current Opinion in Colloid & Interface Science*, *11*(6), 330–336.

Hamman, J. H. (2010). Chitosan based polyelectrolyte complexes as potential carrier materials in drug delivery systems. *Marine Drugs*, *8*(4), 1305–1322.

Hartig, S. M., Greene, R. R., Dikov, M. M., Prokop, A., & Davidson, J. M. (2007). Multifunctional nanoparticulate polyelectrolyte complexes. *Pharmaceutical Research*, *24*(12), 2353–2369.

Ichikawa, S., Iwamoto, S., & Watanabe, J. (2005). Formation of biocompatible nanoparticles by self-assembly of enzymatic hydrolysates of chitosan and carboxymethyl cellulose. *Bioscience Biotechnology and Biochemistry*, *69*(9), 1637–1642.

Kabanov, V. A., & Zezin, A. B. (1984). A new class of complex water-soluble polyelectrolytes. *Die Makromolekulare Chemie*, *6*(S19841), 259–276.

Kabanov, A. V., Bronich, T. K., Kabanov, V. A., Yu, K., & Eisenberg, A. (1996). Soluble stoichiometric complexes from poly(*N*-ethyl-4-vinylpyridinium) cations and poly(ethylene oxide)-block-polymethacrylate anions. *Macromolecules*, *29*, 6796–6802.

Lankalapalli, S., & Kolapalli, V. R. M. (2009). Polyelectrolyte complexes: A review of their applicability in drug delivery technology. *Indian Journal of Pharmaceutical Sciences*, *71*(5), 481–487.

Mihai, M., Dragan, E. S., Schwarz, S., & Janke, A. (2007). Dependency of particle sizes and colloidal stability of polyelectrolyte complex dispersions on polyanion structure and preparation mode investigated by dynamic light scattering and atomic force microscope. *Journal of Physical Chemistry B*, *111*(29), 8668–8675.

Muzzarelli, R. A. A., Greco, F., Busilacchi, A., Sollazzo, V., & Gigante, A. (2012). Chitosan, hyaluronan and chondroitin sulfate in tissue engineering for cartilage regeneration: A review. *Carbohydrate Polymers*, *89*(3), 723–739.

Popa-Nita, S., Alcouffe, P., Rochas, C., David, L., & Domard, A. (2009). Continuum of structural organization from chitosan solutions to derived physical forms. *Biomacromolecules*, *11*(1), 6–12.

Schatz, C., Domard, A., Viton, C., Pichot, C., & Delair, T. (2004). Versatile and efficient formation of colloids of biopolymer-based polyelectrolyte complexes. *Biomacromolecules*, *5*(5), 1882–1892.

Schatz, C., Lucas, J. M., Viton, C., Domard, A., Pichot, C., & Delair, T. (2004). Formation and properties of positively charged colloids based on polyelectrolyte complexes of biopolymers. *Langmuir*, *20*(18), 7766–7778.

Schatz, C., Viton, C., Delair, T., Pichot, C., & Domard, A. (2003). Typical physicochemical behaviors of chitosan in aqueous solution. *Biomacromolecules*, *4*(3), 641–648.

Spruijt, E., Cohen Stuart, M. A., & van der Gucht, J. (2013). Linear viscoelasticity of polyelectrolyte complex coacervates. *Macromolecules*, *46*(4), 1633–1641.

Ueno, K., & Kina, K. y. (1985). Colloid titration – A rapid method for the determination of charged colloid. *Journal of Chemical Education*, *62*(7), 627.

Vachoud, L., Zydowicz, N., & Domard, A. (1997). Formation and characterisation of a physical chitin gel. *Carbohydrate Research*, *302*(3–4), 169–177.

Weber, C., Drogoz, A., David, L., Domard, A., Charles, M.-H., Verrier, B., et al. (2010). Polysaccharide-based vaccine delivery systems: Macromolecular assembly, interactions with antigen presenting cells, and in vivo immunomonitoring. *Journal of Biomedical Materials Research Part A*, *93A*(4), 1322–1334.

Yan, M., Fresnais, J., & Berret, J. F. (2010). Growth mechanism of nanostructured superparamagnetic rods obtained by electrostatic co-assembly. *Soft Matter*, *6*(9), 1997–2005.